Electronic Supporting Information (ESI)

Reversible Twisting-Induced Crystalline–Polycrystalline Transformation in Cyanoacrylate Crystals

Thiyagaraj Parthasarathy,[a] *Aritra Bhowmik,*[b,c] *Biswajit Bhattacharya,*[d] *Manish Kumar Mishra,**[b,c] *Soumyajit Ghosh**[a]

[a]Department of Chemistry, SRM Institute of Science and Technology, Kattankulathur 603 203, Tamil Nadu, India.

[b]Physical and Materials Chemistry Division, CSIR-National Chemical Laboratory, Pune 411008, India.

[c]Academy of Scientific and Innovative Research (AcSIR), Ghaziabad-201002, India.

[d]BAM Federal Institute for Materials Research and Testing, Richard-Willstätter-Str. 11, 12489 Berlin, Germany.

* Email: soumyajitghosh89@gmail.com (SG)

Email: mishra_mani07@yahoo.in and mk.mishra.ncl@csir.res.in (MKM)

Table of Contents:

Serial No.	Title	Page No.
1	Materials	S3
2	Instrumental Methods	S3-S4
3	Synthesis of compounds **1** and **2**	S4-S5
4	Figure S1: ^{1}H NMR spectrum of crystal **1**	S6
5	Figure S2: ^{1}H NMR spectrum of crystal **2**	S7
6	Table S1: Crystallization table	S7-S8
7	Table S2: Crystallographic data of crystals **1** and **2**	S8-S9
8	Figure S3: Face Indexing of crystal **1** and crystal **2**	S9
9	Figure S4: Elastic strain calculation	S10
10	Figure S5: Structural packing of crystals **2**	S10-S11
11	Figure S6: Hirshfeld analysis	S11-S12
12	Figure S7-S8: Stepwise elastic images	S12
13	Figure S9: Crystal packing of plastic deformation of crystal **2**	S13
14	Figure S10: Elastic strain calculation after twisting	S13
15	Figure S11-13: Images show a number of pitches in a twisted crystal.	S14-S15
16	Figure S14: Schematic representation of crystal **2**	S15
17	Figure S15: FESEM images of crystals **1** and **2**	S16
18	Figure S16: Single crystal X-ray diffraction frames for crystal **1** and crystal **2**	S16
19	Figure S17: PXRD analysis of crystals **1** and **2**	S17
20	Figure S18: Micro-focus Raman Spectra of Crystal **1**, pristine, twisted, and untwisted crystal.	S17
21	Figure S19: Micro-focus Raman Spectra of Crystal **2**, pristine, twisted, and untwisted crystal.	S18

1. Experimental Section

1.1 Materials

The compounds ethyl 2-cyanoacetate and 4-chlorobenzaldehyde, 3,4-chlorobenzaldehyde were purchased from Spectrochem and Avra for synthesis purposes. Commercially available solvents were used as received without further purification for crystallization.

1.2 NMR spectroscopy studies: ^{1}H NMR spectra were recorded using a Bruker Advance III spectrometer at 500 MHz. The $CDCl_3$ solvent system was used to record the spectra. ^{1}H NMR spectra were collected under standard conditions. Chemical shifts (δ) are reported in parts per million (ppm).

1.3 Single crystal X-ray diffraction: Single crystal data for **1** and **2** were collected on a Bruker D8 Venture system with graphite monochromatic (Mo Kα, 0.71073 Å) radiation at 300 K. Data reduction was performed using the Bruker AXS SAINT and SADABS programs. The structures were solved by direct methods using SHELXT 2018, followed by successive Fourier and difference Fourier transformations.[1] SHELXL 2013 was used for full-matrix least-squares refinements on F^2.[2] Refinement of coordinates and anisotropic thermal parameters of non-hydrogen atoms was performed using the full-matrix least-squares method. Mercury software was utilized for molecular representations in the ORTEP diagrams. Although the crystal structure of crystal **2** has been reported previously,[3,4] we have successfully reproduced the same structure as part of our study. Detailed data collection, structure refinement, and crystallographic data are shown in Table S2, ESI.

1.4 Powder X-ray diffraction studies: Powder X-ray diffraction (PXRD) patterns were recorded using a Bruker D8 Advance diffractometer equipped with Cu Kα radiation = 1.540 Å. The powdered samples were dried and then analyzed over a 2θ range of 5–50°, with a step

size of 0.02°. Before data collection, the instrument was calibrated using a silicon standard. The X-ray tube was operated at a voltage of 40 kV and a current of 50 mA respectively.

1.5 Differential scanning calorimetry:

Differential scanning calorimetry (DSC) analysis was performed using a Mettler Toledo DSC 822e instrument to measure enthalpy changes. The dried crystals were placed in a 40 μL aluminum pan and securely crimped. The sample was then heated from room temperature (25 °C) to 200 °C at a heating rate of 10 °C min^{-1}, with an empty aluminum pan serving as the reference. Nitrogen gas was used as the purge gas at a flow rate of 40 mL min^{-1}.

1.6 Field emission scanning electron microscopy:

Field Emission Scanning Electron Microscopy (FE-SEM) analysis was performed using an FEI NOVA NANO 450 instrument at an accelerating voltage of 20 kV to achieve ultra-high resolution. The imaging was conducted with a dwell time of 6–10 μs across various magnifications, covering an area range of 200 to 5 μm.

1.7 Raman Spectra of Pristine, Twisted and Untwisted Crystal:

Raman spectra were recorded for straight, twisted, and untwisted forms of Crystal **1** and Crystal **2** using a confocal Raman microscope (TechnoS IndiRAM CTR 500C Micro Raman Spectrometer, India) equipped with a CCD detector. A 532 nm diode laser served as the excitation source. For the straight crystals, a 50× objective lens was used, with spectra collected at an 8-second integration time and averaged over 5 accumulations. For the twisted and untwisted regions, measurements were also taken using the same 50× lens (laser beam diameter: 1 μm), with identical acquisition parameters (8-second integration, 5 accumulations).

2. Synthesis procedure of compound 1 and 2

Compounds **1** and **2** were synthesized using a reported literature by dissolving 3,4-chlorobenzaldehyde (1 mmol) and 4-chlorobenzaldehyde in a 100 ml round bottom-flask containing 15 ml of ethanol, and to the resultant solution ethyl 2-cyanoacetate (1 mmol) was added slowly.[5] The mixture was refluxed for 6 hours and after 6 hours product was precipitated out from the reaction medium. The progress of the reaction was checked periodically using TLC. The obtained precipitate was filtered out and dried off with a decent yield (Compound **1**: ~80% and Compound **2**: ~75%). Crystallization was done by slow evaporation technique at room temperature and single crystals were harvested from hot solvents such as methanol/acetonitrile in 1:1 ratio. Well-diffraction quality crystals appeared from crystallization vessel eight days later.

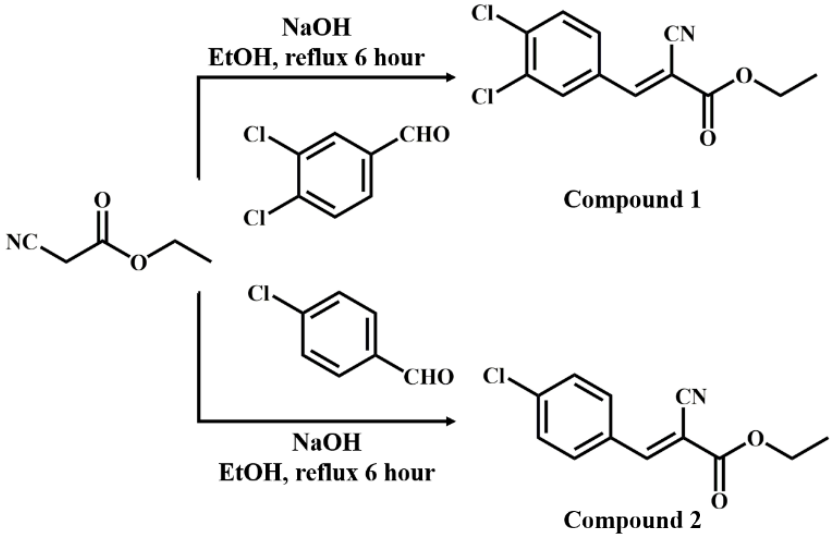

Scheme S1. Synthesis procedure of compound **1** and **2.**

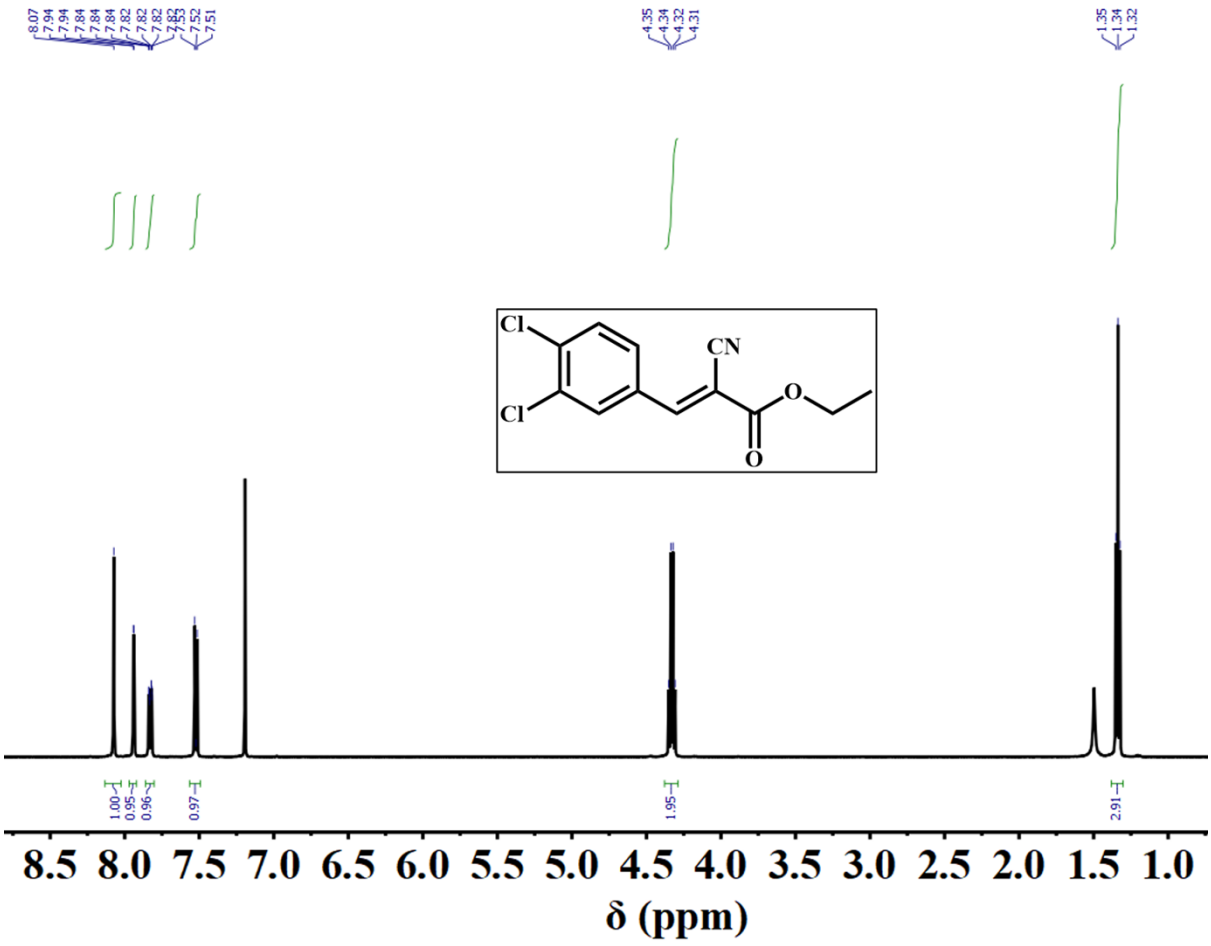

Fig. S1 ^{1}H NMR spectrum of crystal **1** (solvent: $CDCl_3$, peak at 7.26 ppm). Crystal **1**: ^{1}H NMR (500 MHz, Chloroform-*d*) δ 8.07 (s, 1H), 7.94 (d, *J* = 2.2 Hz, 1H), 7.86 – 7.79 (m, 1H), 7.52 (d, *J* = 8.5 Hz, 1H), 4.33 (q, *J* = 7.1 Hz, 2H), 1.34 (t, *J* = 7.1 Hz, 3H).

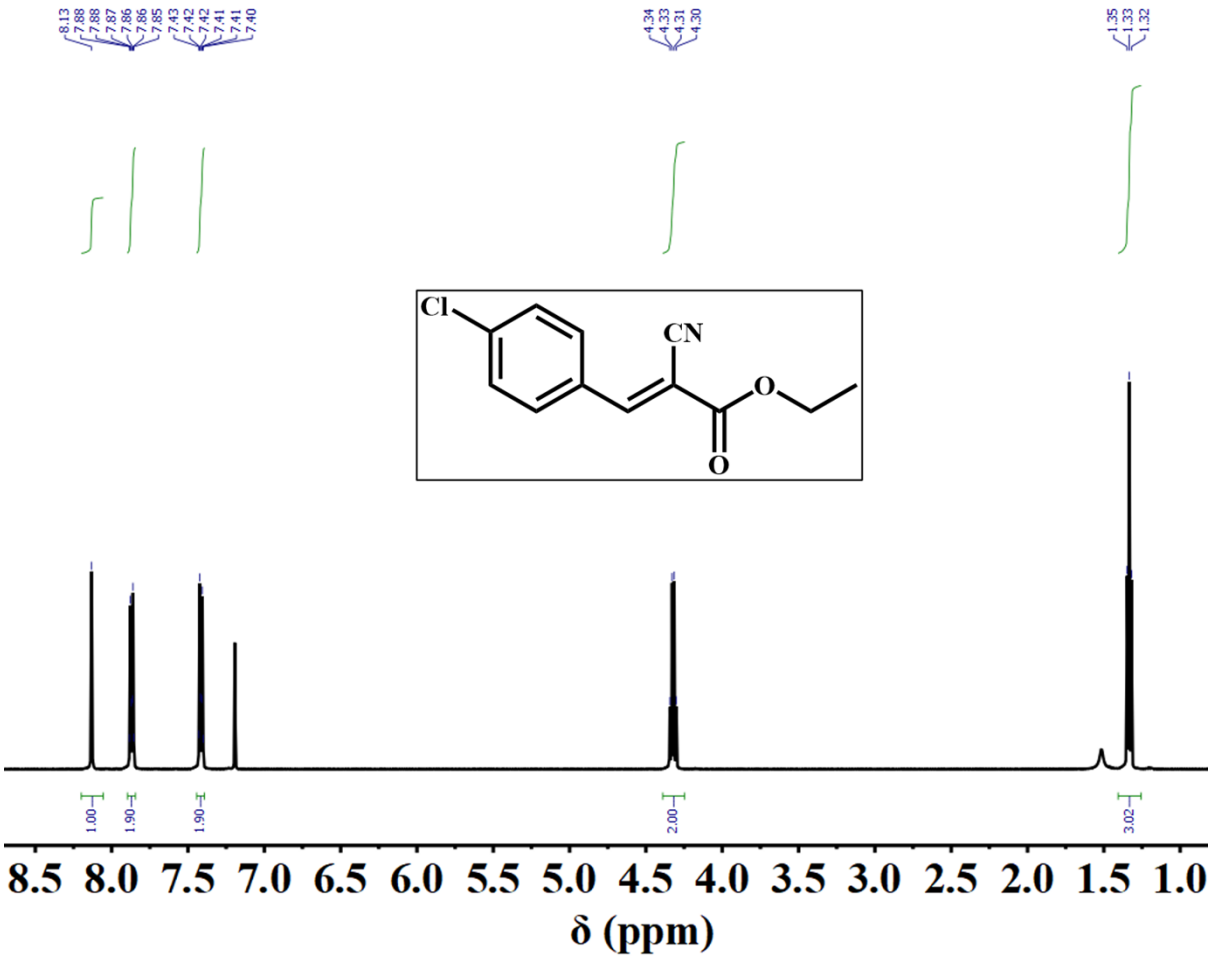

Fig. S2 ^{1}H NMR spectrum of crystal **2** (solvent: $CDCl_3$, peak at 7.26 ppm). Crystal **2**: ^{1}H NMR (500 MHz, Chloroform-*d*) δ 8.13 (s, 1H), 7.90 – 7.84 (m, 2H), 7.44 – 7.39 (m, 2H), 4.32 (q, J = 7.1 Hz, 2H), 1.33 (t, J = 7.1 Hz, 3H).

Table S1: Results from the crystallization of compounds 1 and 2 from one solvent or mixture of solvents.

S.No.	Solvents	Compound 1	Compound 2
1.	Ethyl Acetate + n-Hexane (1:1)	Powder	Powder
2.	Dichloromethane + Methanol (1:1)	Powder	Powder

3.	Ethyl Acetate + Methanol (1:1)	Powder	Powder
4.	Ethyl Acetate + n-Hexane (1:1)	Powder	Powder
5.	Acetonitrile	Powder	Needles
6.	Methanol + Acetonitrile	Fine needles	Fine needles
7.	Chloroform	Powder	Powder

Table S2: Crystallographic Information Table of Crystals 1 and 2.

Compound	**Crystal 1**	**Crystal 2**
Formula	$C_{12}H_9Cl_2NO_2$	$C_{12}H_{10}ClNO_2$
Molecular weight	270.10	235.66
T/K	299	300
Crystal system	monoclinic	monoclinic
Space group	$P2_1/n$	$P2_1/n$
a (Å)	14.659(3)	14.959(4)
b (Å)	5.5305(10)	5.3671(12)
c (Å)	16.434(4)	15.422(4)
α (°)	90	90
β (°)	110.704(8)	108.397(10)
γ (°)	90	90
Volume/Å^3	1246.3(4)	1174.9(5)
Z	4	4
ρ_{calc}, g/cm^{-3}	1.440	1.332
μ /mm^{-1}	0.508	0.309
F(000)	552.0	488.0
2Θ range/^{o}	5.3 to 53.538	5.568 to 52.818
Index ranges	$-18 \leq h \leq 18$, $-6 \leq k \leq 6$, $-20 \leq l \leq 20$	$-18 \leq h \leq 18$, $-6 \leq k \leq 6$, $-18 \leq l \leq 18$
Crystal Size/mm^3	0.42 × 0.2 × 0.1	0.42 × 0.2 × 0.1
Reflections collected	14099	16249

Independent Reflections	2603	2191
R_{int}	0.0410	0.0616
Goodness-of fit (F^2)	1.043	1.031
Data completeness	0.984	0.911
Final *R* indexes [I>=2σ (I)]	R1 = 0.0451 wR2 = 0.1178	R1 = 0.0446 wR2 = 0.1109
Final *R* indexes [all data]	R1 = 0.0640 wR2 = 0.1381	R1 = 0.0672 wR2 = 0.1243
CCDC Number	2446157	2446156

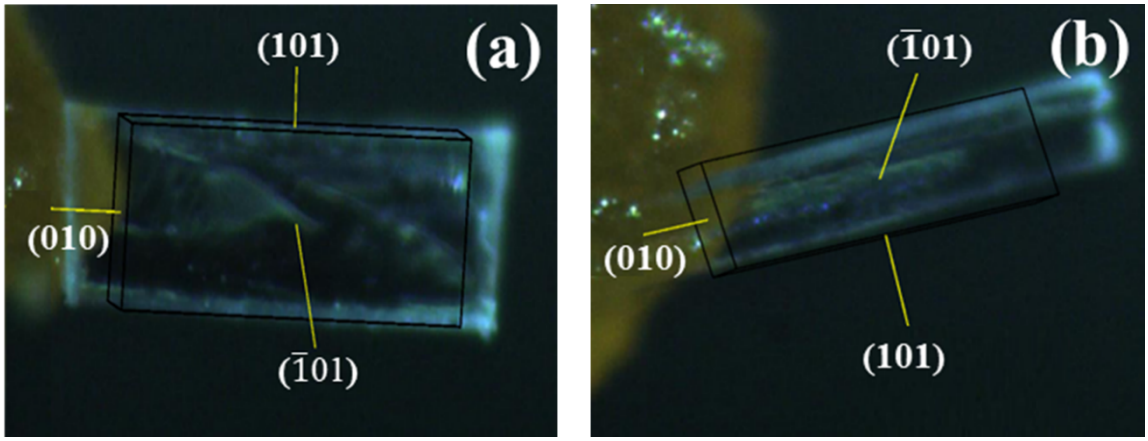

Fig. S3 Face Indexing of Crystal **1** and Crystal **2**.

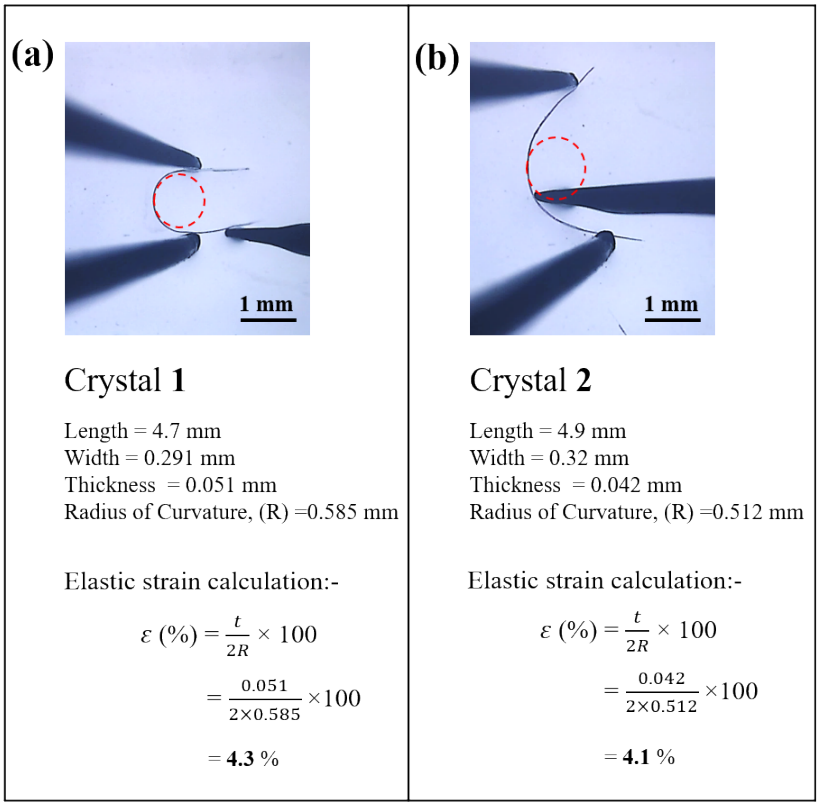

Fig. S4 Elastic strain calculation of the crystals **1** (a) and **2** (b).

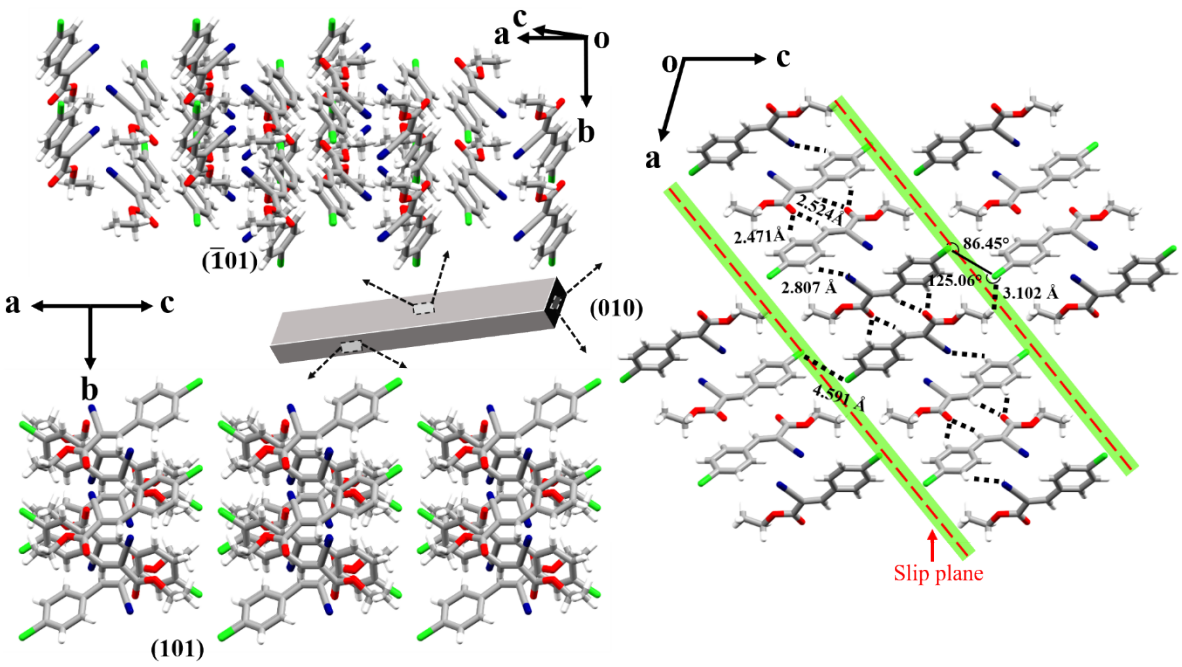

Fig. S5 Crystal packing view of crystal **2** viewed from ($\bar{1}$01), (010) and (101) faces show various interactions and their respective distances.

Crystals of **2** were grown with space group $P2_1/n$ with Z = 4. Packing analysis of **2** shows that two molecules are connected to form centrosymmetric dimers *via* bifurcating C–H···O interactions (2.47(3) Å and 2.52(3) Å). Neighboring centrosymmetric dimers are connected *via* C–H···N interactions (2.80(2) Å) to form a zigzag extended 1D tape along [101] direction. Zigzag tapes are sustained by π···π interactions along *b* axis to form 2D corrugated sheets in ($\bar{1}$01) plane. Neighboring 2D sheets are interconnected mainly by three interactions quasi type II Cl···Cl (4.59 (3) Å, 86.45(2)°, 125.06(4)°), C–H···Cl interaction (3.10(4) Å) and Me···Me van der Waals interactions.

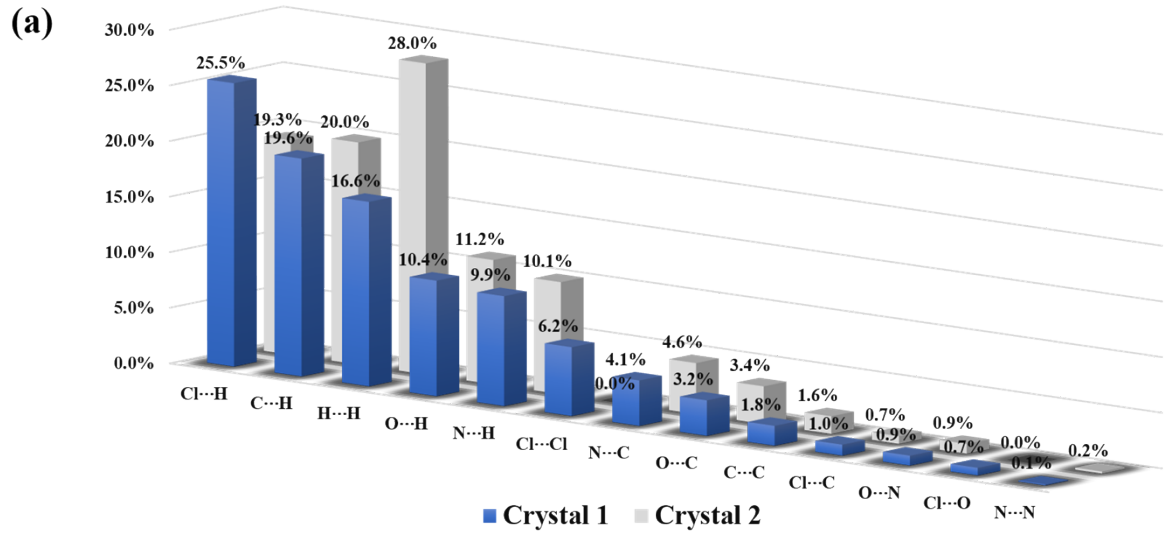

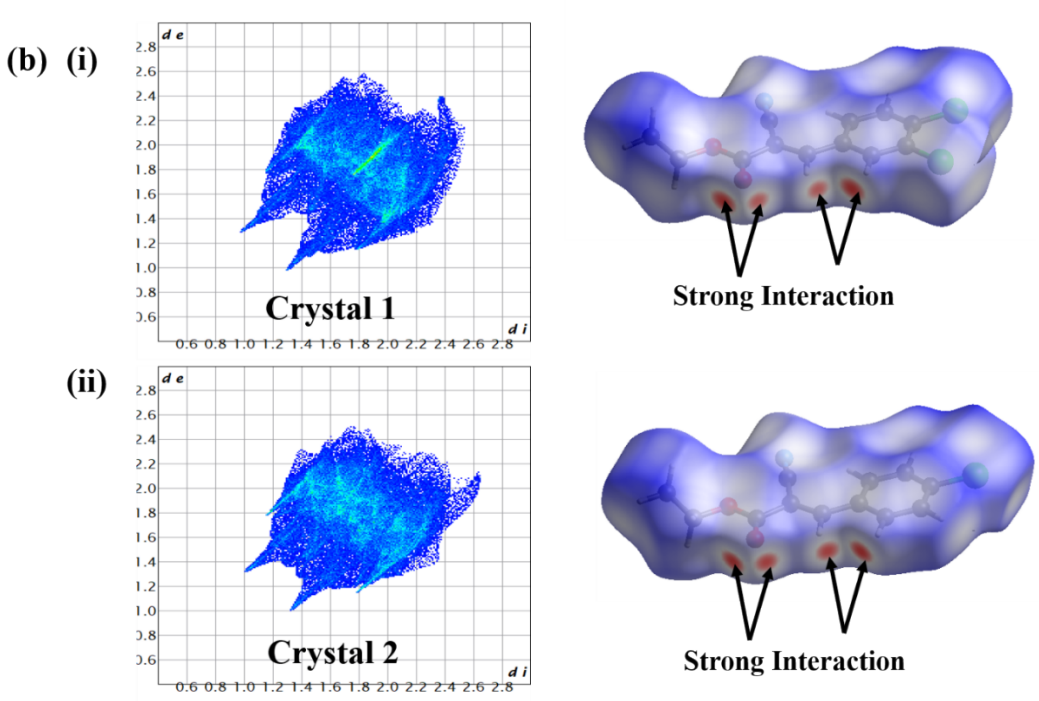

Fig. S6 The relative contribution of intermolecular interactions to the Hirshfeld surface area (a) shows percentage of individual atomic contact contributions to the Hirshfeld surface of crystals **1** and **2**, (b) fingerprint plots of crystals **1** and **2**.

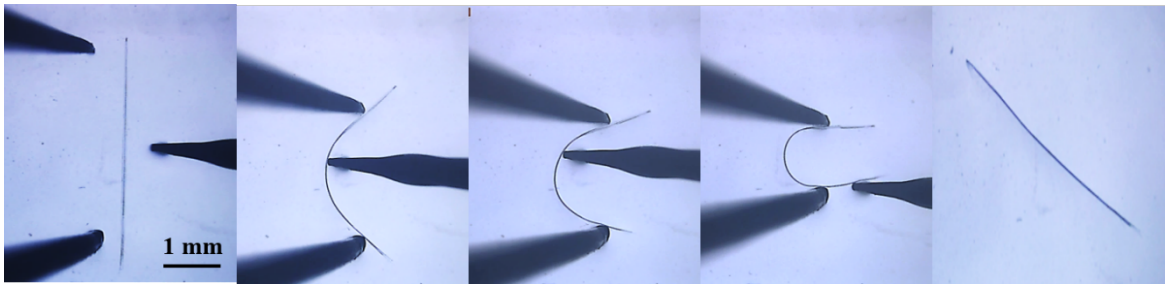

Fig. S7 Stepwise elastic bending cycles of crystal **1.**

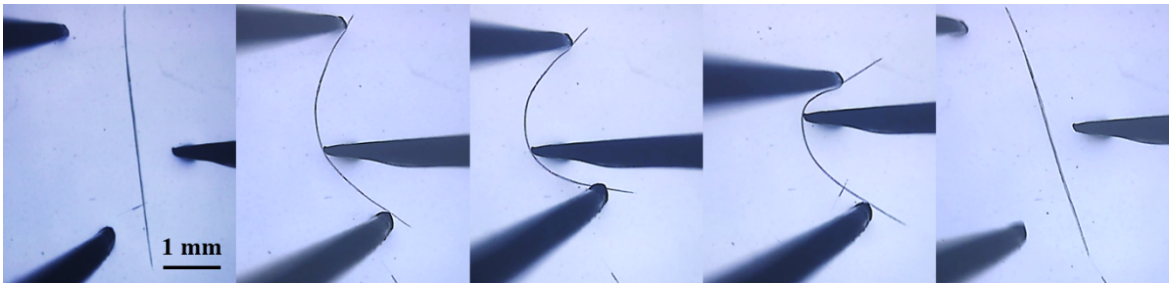

Fig. S8 Stepwise elastic bending cycles of crystal **2.**

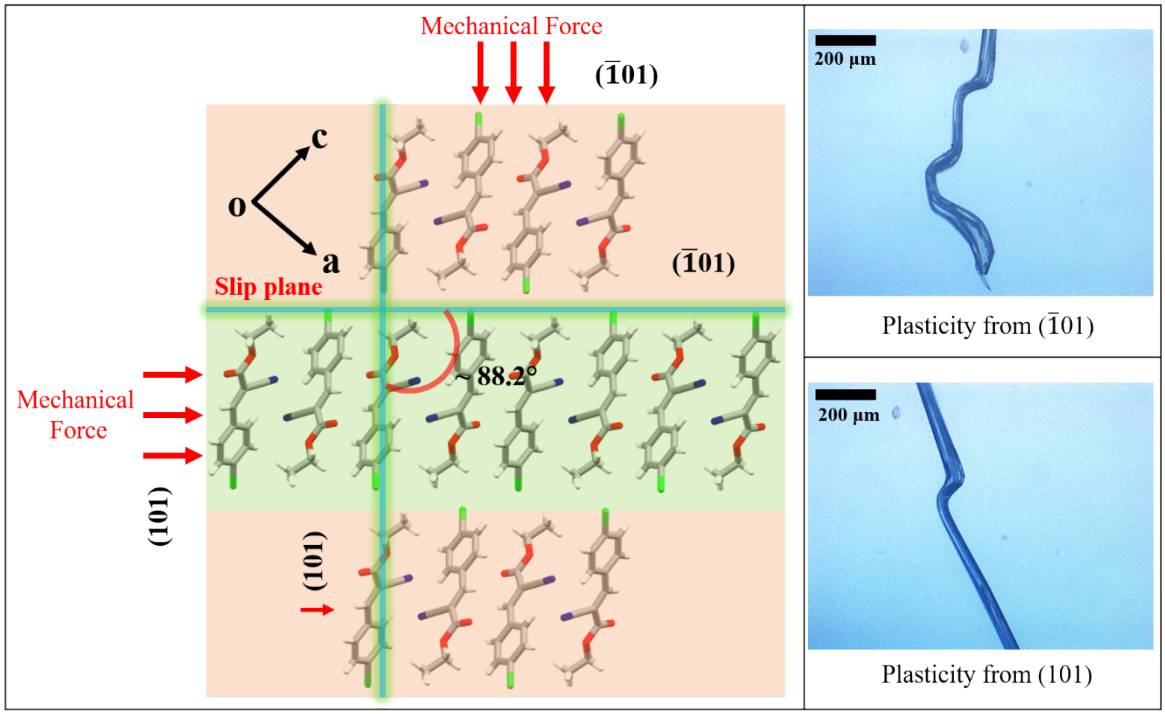

Fig. S9 Crystal packing shows mechanical stress direction applied from ($\bar{1}$01) and (101) faces for crystal **2**.

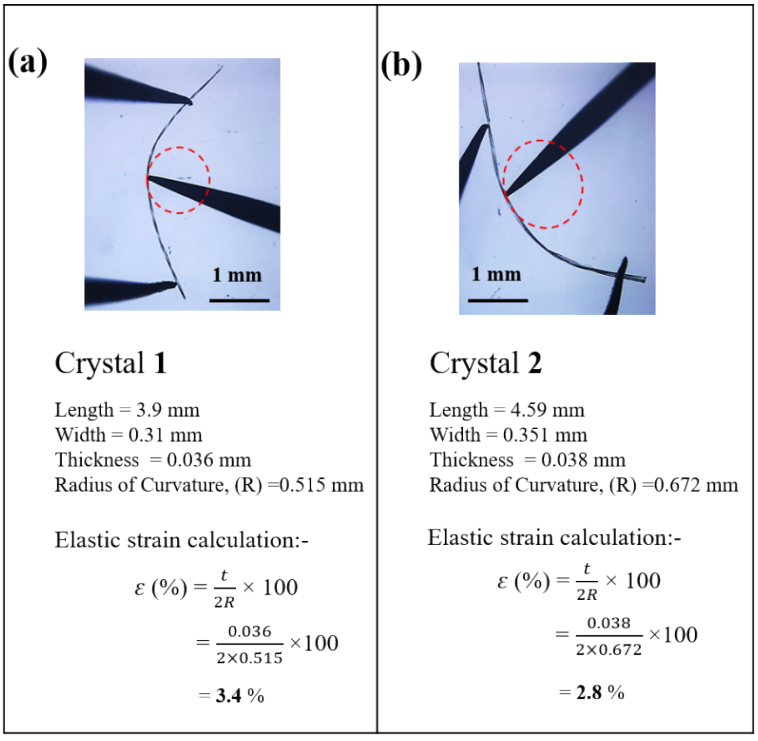

Fig. S10 Elastic strain calculation of the crystals **1** (a) and **2** (b) after twisting.

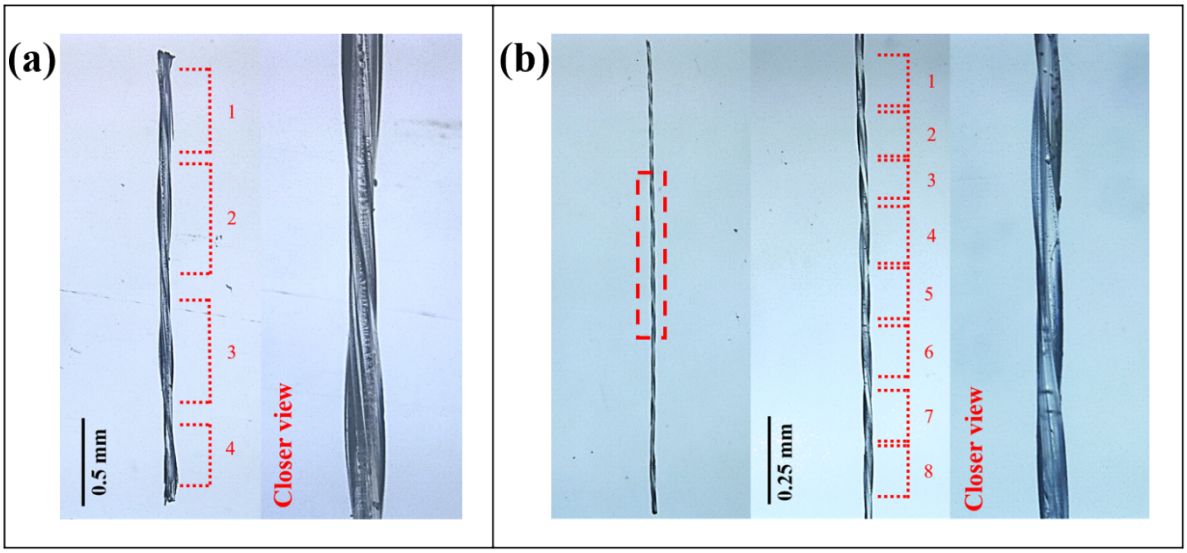

Fig. S11 (a) and (b) shows the minimum and the maximum number of twists depending on the extent of twist force on crystal **1**.

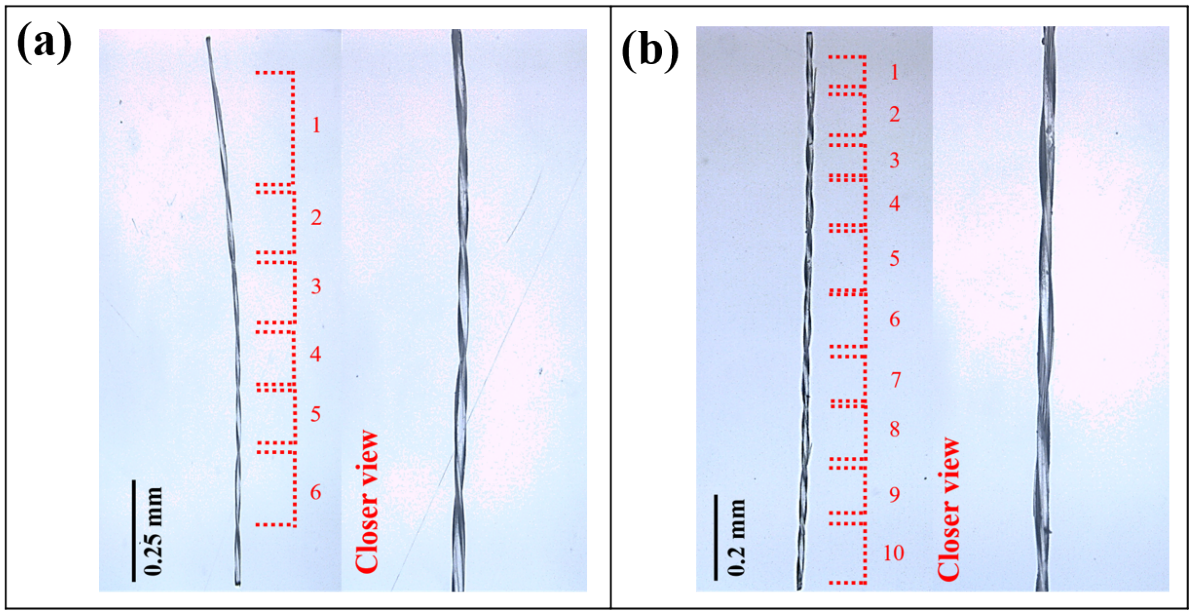

Fig. S12 (a) and (b) shows the minimum and maximum number of twists depend on the extent of twist force on crystal **2**.

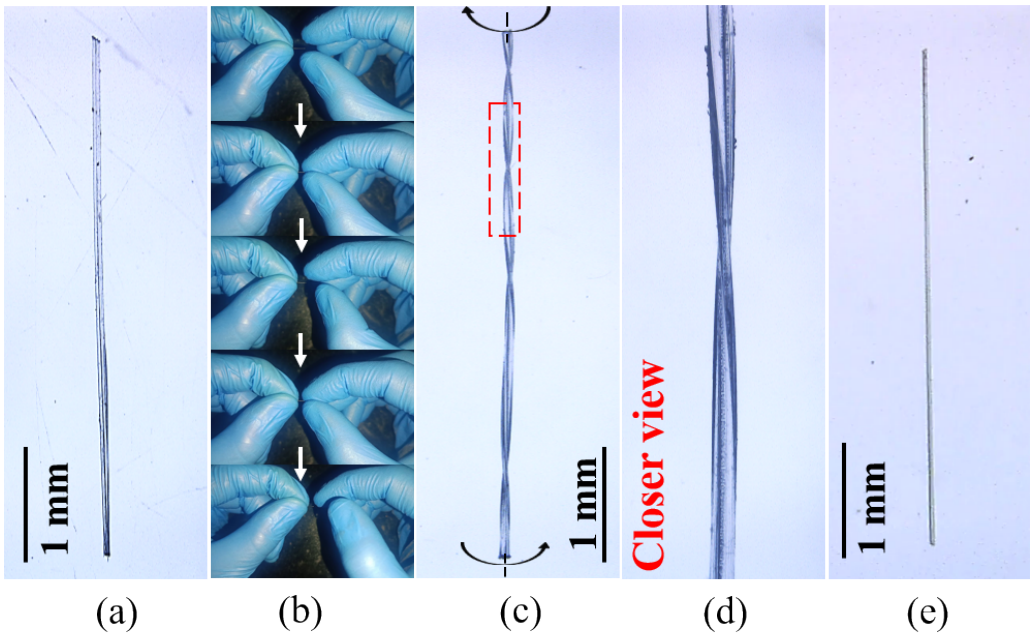

Fig. S13 (a) Straight crystal **2** before applying twist force. (b) and (c) Stepwise twisting of crystal **2** by hand. (d) Enlarged view of the hand-twisted crystal **2**. (e) Straightened crystal image of crystal **2** through reversible twist by hand.

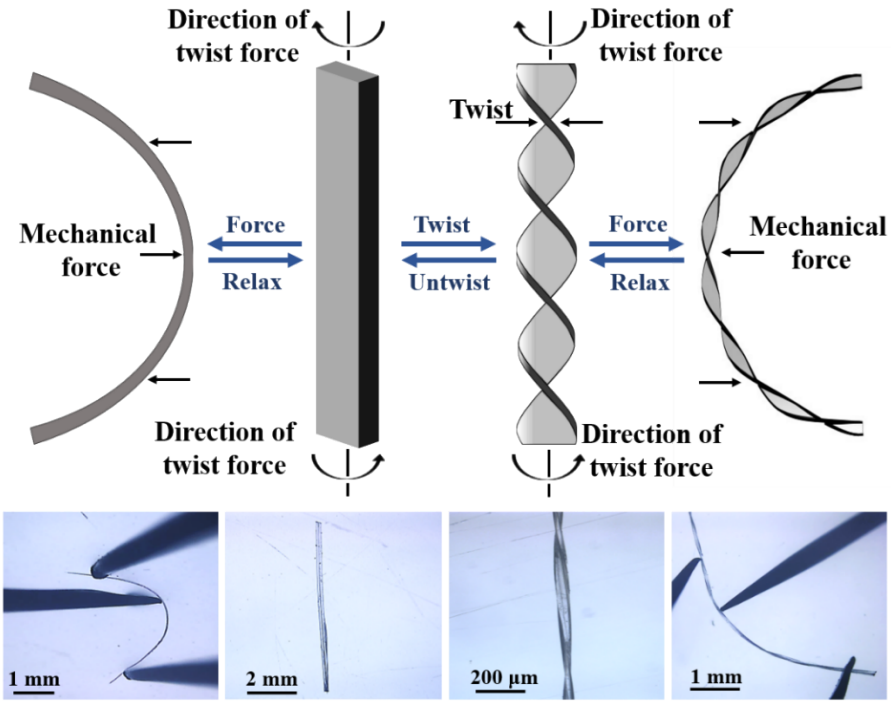

Fig. S14 Schematic representation of elasticity and reversible twisting of crystal **2**.

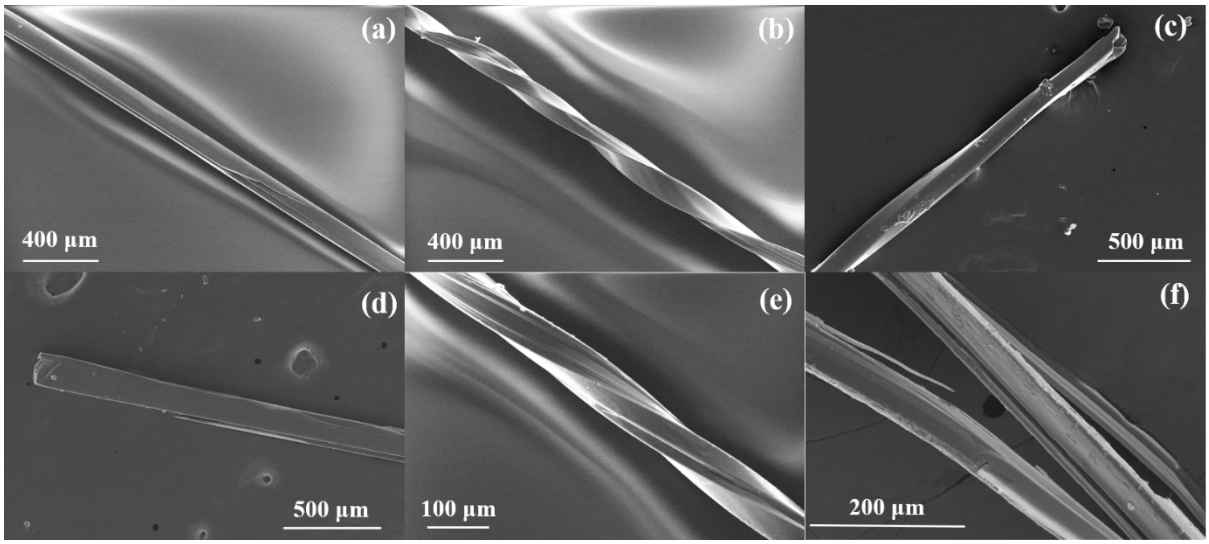

Fig. S15 FESEM images of crystals **1** and **2**: straight crystal (a) and (d), twisted crystal (b) and (e), untwisted crystal (c) and (f).

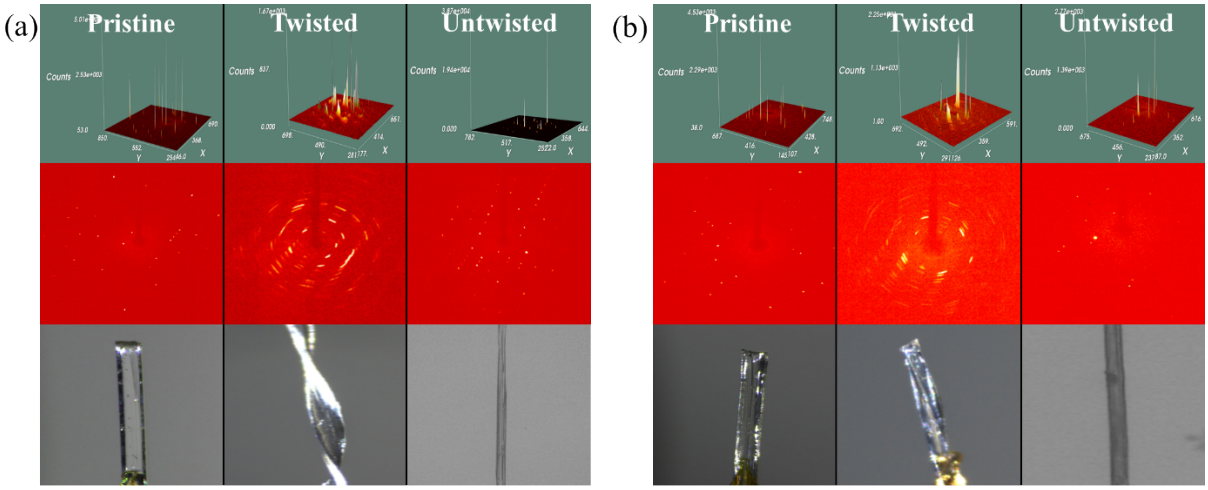

Fig. S16 Representative single crystal X-ray diffraction frames for a pristine, twited and untwisted crystal of (a) Crystal **1** and (b) Crystal **2**.

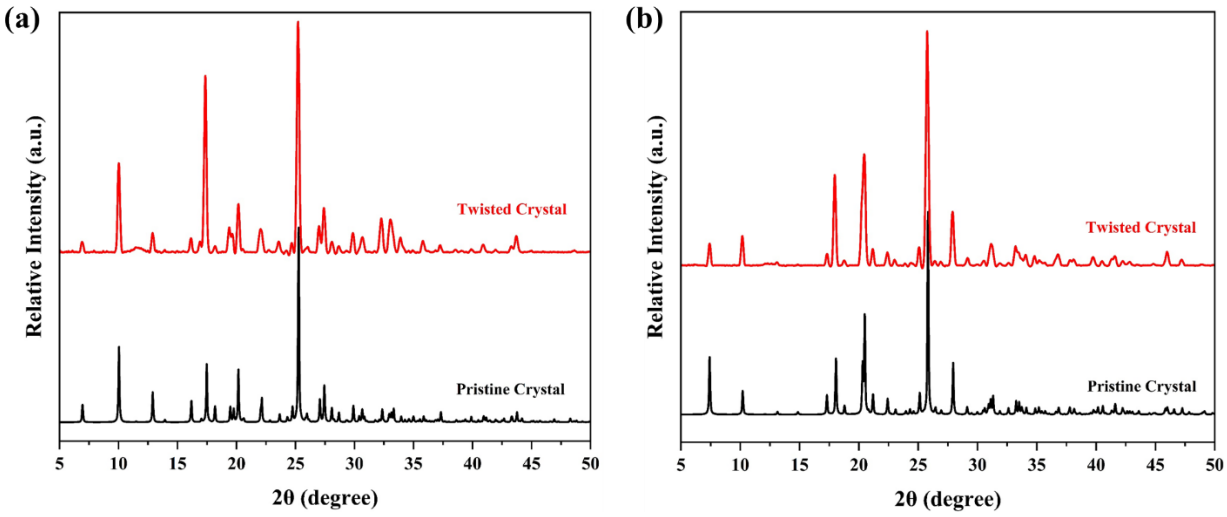

Fig. S17 (a) and (b) shows crystal **1** and **2** pristine and twisted PXRD profile comparison.

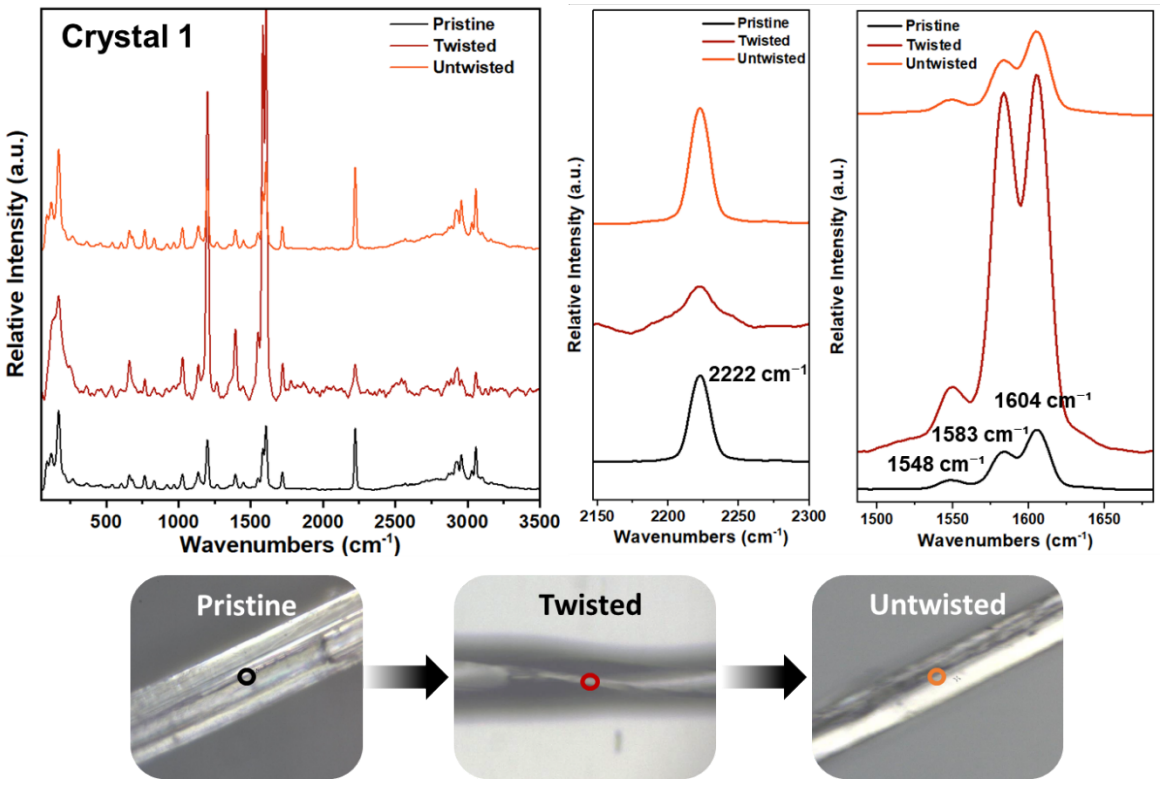

Fig. S18 Micro-focus Raman Spectra of Crystal **1,** pristine, twisted, and untwisted crystal.

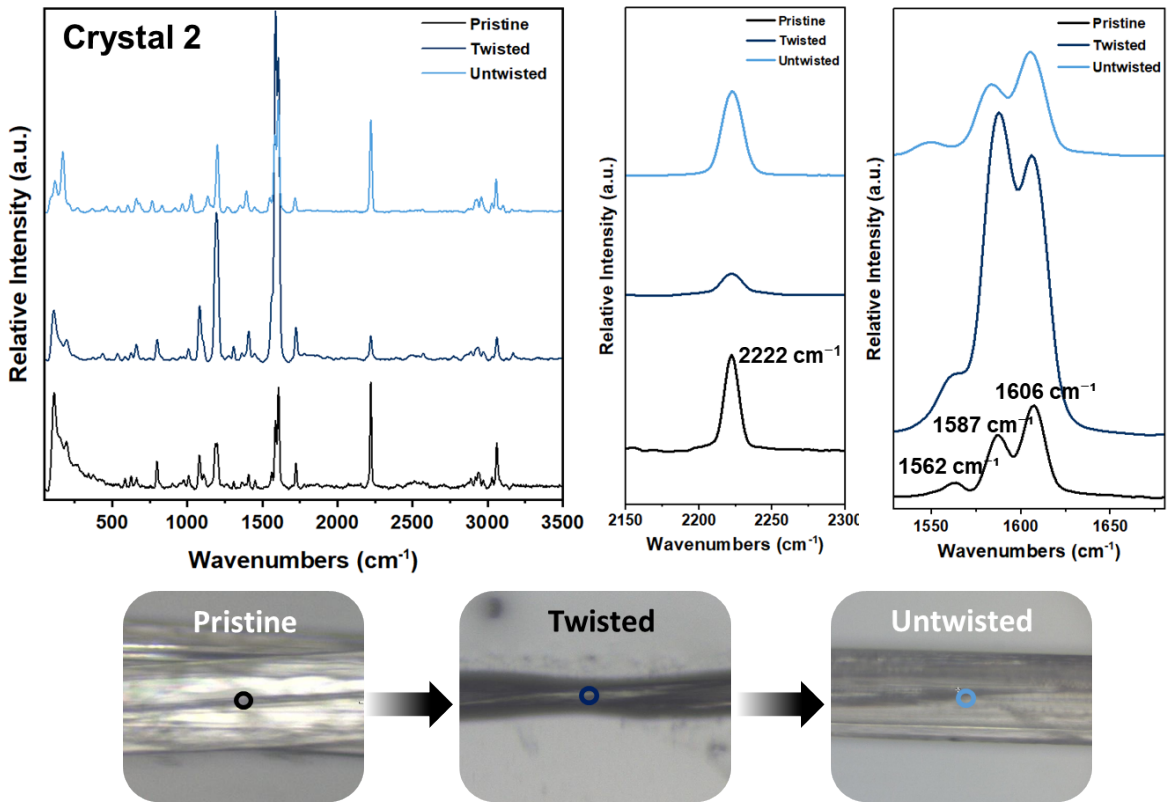

Fig. S19 Micro-focus Raman Spectra of Crystal **2,** pristine, twisted, and untwisted crystal.

References:

1. G. M. Sheldrick, *Acta Crystallogr., Sect. A,* 2008, **64**, 112–122.
2. G. M. Sheldrick, *Acta Crystallogr., Sect. A,* 2015, **71**, 3–8.
3. A. Mishra, P. Yadav and S. K. Awasthi, *ACS Org. Inorg. Au,* 2023, **3**, 254-265.
4. Y. Zhang and J. W. Liu, *Acta Crystallogr., Sect. E,* 2006, **62**, o5286–o5287.
5. H. Yasuda and H. Midorikawa, *Bull. Chem. Soc. Jpn.,* 1966, **39**, 1754–1759.